Epigenetic QTL Mapping in *Brassica napus*

Yan Long,*,[1] Wei Xia,*,[1] Ruiyuan Li,* Jing Wang,* Mingqin Shao,* Ji Feng,* Graham J. King,[†]
and Jinling Meng*,[2]

*National Key Laboratory of Crop Genetic Improvement, Huazhong Agricultural University, Wuhan 430070, China
and [†]Southern Cross Plant Science, Southern Cross University, Lismore, NSW 2480, Australia

ABSTRACT There is increasing evidence that epigenetic marks such as DNA methylation contribute to phenotypic variation by regulating gene transcription, developmental plasticity, and interactions with the environment. However, relatively little is known about the relationship between the stability and distribution of DNA methylation within chromosomes and the ability to detect trait loci. Plant genomes have a distinct range of target sites and more extensive DNA methylation than animals. We analyzed the stability and distribution of epialleles within the complex genome of the oilseed crop plant *Brassica napus*. For methylation sensitive AFLP (MSAP) and retrotransposon (RT) epimarkers, we found a high degree of stability, with 90% of mapped markers retaining their allelic pattern in contrasting environments and developmental stages. Moreover, for two distinct parental lines 97% of epialleles were transmitted through five meioses and segregated in a mapping population. For the first time we have established the genetic position for 17 of the 19 centromeres within this amphidiploid species. Epiloci and genetic loci were distributed within distinct clusters, indicating differential detection of recombination events. This enabled us to identify additional significant QTL associated with seven important agronomic traits in the centromeric regions of five linkage groups.

DNA methylation is a modification of DNA sequence that serves to repress the influence of transposable elements (TEs) and other repetitive sequences within the eukaryote genomes of fungi, plants, and animals (Martienssen and Colot 2001). Cytosine methylation (5mC), catalyzed by DNA methyltransferases, may also lead to heritable and/or reversible changes in chromatin structure and gene expression that do not entail changes in nucleotide sequence (Finnegan *et al.* 2000; Martienssen and Colot 2001).

DNA methylation in plant nuclear genomes was initially thought to occur predominantly in the cytosines of symmetrical sequences such as CG and CHG, with up to 20–40% of all cytosine residues being methylated (Gruenbaum *et al.* 1981; Messeguer *et al.* 1991). However, the level of 5mC varies considerably across plant taxa, with early estimates indicating 6% of cytosines methylated in *Arabidopsis* (Kakutani *et al.* 1999), 24% of potential methylation sites

in *B. oleracea* (Kovarik *et al.* 1997), and up to 25% in maize (Papa *et al.* 2001). More recently, whole genome bisulfite sequencing at base-pair resolution in *Arabidopsis* (Lister *et al.* 2008) has shown that 5.26% of all genomic cytosines are methylated and unevenly distributed in the genome, with the majority in the CG context (55%), followed by CHG (23%), and CHH (22%). Heavy methylation is observed in the centromere and pericentromeric region (Zilberman *et al.* 2007; Lister *et al.* 2008; Yan *et al.* 2010). Transposable elements and sequences flanking insertion sites are typically methylated, suppressing transposon activity, especially in centromeres and pericentromeric regions where abundant TEs insert (Slotkin and Martienssen 2007; Zilberman *et al.* 2007; Han *et al.* 2010).

Across most eukaryote taxa, DNA methylation plays an important role in controlling gene expression (Suzuki and Bird 2008) and phenotype, including human disease (Robertson 2005; Watanabe and Maekawa 2010) and plant development (Kalisz and Purugganan 2004; King *et al.* 2010). In higher plants, genome-wide decreased DNA methylation can alter flowering time (Horváth *et al.* 2002; Kondo *et al.* 2006) and specific epialleles may result in phenotype variation in different crops. For example, in tomato, a hypermethylated allele of an SBP-box gene *LeSPL* reduces its expression in epimutant fruits, leading to inhibition of ripening

(Manning *et al.* 2006). During *Arabidopsis* seed development >50 genes are imprinted in the female tissue, with corresponding hypomethylation in the endosperm in addition to the well-described imprinted genes *FWA*, *MEA*, *FIE*, and *FIS2* (Gehring *et al.* 2009). Also in *B. rapa*, the epiallele of *SP11* is involved in the dominance interaction that determines the self-incompatibility phenotype (Shiba *et al.* 2006).

Although there is increasing evidence that phenotype is influenced by epigenetic marks playing a key role in regulating gene transcription, developmental plasticity, and interactions with the environment, relatively little is known about the relationship between the distribution of DNA methylation within chromosomes and the ability to detect trait loci. A first step is to determine the chromosomal distribution of 5mC and how this may affect the detection of recombination events in segregating populations.

The *B. rapa* genome is estimated to be 480–520 Mb and to contain 40–50% repeat sequences, including TEs in the euchromatin region (14%) and repeat sequences in the large centromeric region (30%) (Johnston *et al.* 2005; Lim *et al.* 2005; Hong *et al.* 2006). A recent cytological study has suggested a distinct distribution of DNA methylation, primarily located in the heterochromatin, when compared with *B. oleracea* (Braszewska-Zalewska *et al.* 2010), which diverged from *B. rapa* ∼3.7 MYA (Inaba and Nishio 2002) and shares a common complex pattern of triplicated segments arising from a series of ancestral duplication events (Yang *et al.* 2006). A high rate of DNA methylation (52–60%) has been found in different accessions of *B. oleracea*, detected by the methylation-sensitive amplification polymorphism (MSAP) method, with most of the MSAP fragments stably inherited through meiosis (Salmon *et al.* 2008).

B. napus is a stable amphidiploid oil crop of major economic significance (canola, oilseed rape), derived from a recent hybridization between *B. rapa* and *B. oleracea* (Allender and King 2010). We have previously mapped hundreds of QTL controlling dozens of important agronomic traits on a *B. napus* reference genetic map (BnTNDH) (Qiu *et al.* 2006; Long *et al.* 2007; Shi *et al.* 2009). Here we report the detection of DNA methylation loci that enabled construction of an epigenetic map, based on MSAP, retrotransposon-specific, and centromeric-specific markers. This enabled the resolution of epi-QTL that were distinct from genetic QTL within the context of an integrated map.

Materials and Methods

Phenotyping and epigenotyping

The reference BnTNDH mapping population has been described previously (Qiu *et al.* 2006). Phenotypic data for seven traits associated with yield, seed quality, and plant development were collected from between 2 to 10 environments in the field during 2002–2007 (Long *et al.* 2007; Shi *et al.* 2009) and used for QTL identification (Table S1). Fully expanded leaves 5–6 from seedlings, and young flower buds at budding stage were sampled to extract genomic DNA.

Two sets of epigenetic markers (epimarkers) were used for epigenotyping the DNA methylation status of the mapping population and parents. (1) MSAP markers, which have been used to detect CG and CHG site methylation variation in a range of genomes (Reyna-Lopez *et al.* 1997; Vuylsteke *et al.* 1999). For CG site methylation detection, restriction enzyme combinations *Eco*RI/*Hpa*II and *Eco*RI/*Msp*I were used, and *Pst*I/*Mse*I for CHG. (2) Two subclasses of retrotransposon-specific markers: (a) genome-wide retrotransposons (RTg) that detect transposons such as TRIM (Kwon *et al.* 2007) and SINE (Prieto *et al.* 2005) were detected by a sequence-specific amplification polymorphism (SSAP) approach (Waugh *et al.* 1997; Ellis *et al.* 1998) and (b) centromere-specific retrotransposons (RTc) that detect transposons clustered within cetromeric regions. Primers were designed on the basis of centromere-specific sequences within *B. rapa* (Lim *et al.* 2007), with insertion–deletion detected by PCR (Figure 1A; Table S2).

Linkage map construction and QTL resolution

Three linkage maps were constructed and designated as epigenetic map (E-map), genetic map (G-map), and integrated map (I-map). Epimarkers were used to construct the E-map, which was superimposed on the framework of the existing well-defined G-map (Shi *et al.* 2009). This enabled epimarkers to be anchored within the context of stable genetic markers that define the established 19 linkage groups and chromosomes of *B. napus*. A revised conventional G-map was developed on the basis of genetic markers (genmarkers) that included RFLP, SSR, and STS mostly used in previous studies (Long *et al.* 2007; Shi *et al.* 2009). Maps were constructed using JoinMap 4.0 (Van Ooijen 2006) with default parameters and linkage groups distinguished at LOD values between 8 and 19. On the basis of the markers common to the E- and G-maps, BioMercator 2.0 software (http://www.generationcp.org/) was used to generate the I-map.

Phenotypic data from each environment (Long *et al.* 2007; Shi *et al.* 2009) were used to identify and map QTL within the three linkage maps (*i.e.*, E-map, G-map, and I-map). Composite interval mapping (CIM) within WinQTL-Cart 2.5 (Wang *et al.* 2006) was used with a significance threshold of $P = 0.05$ using the permutation test method, based on 1000 runs of randomly shuffling the trait values (Churchill and Doerge 1994). QTL identified in different experiments for each trait (primary QTL) were integrated into consensus QTL by the meta-analysis method (Shi *et al.* 2009) (BioMercator 2.0, http://www.generationcp.org/).

Chromosome fluorescent in situ hybridization analysis

A total of 110 *B. napus* BAC clones were selected using a *B. rapa* centromere BAC (AC166739) as the query sequence in BLASTN alignments with TapidorDH BAC-end sequences within GenBank (http://www.ncbi.nlm.nih.gov/sites/entrez?db=nucleotide). Following PCR with RTc marker primers, clone

Table 1 Variation in DNA methylation status for MSAP markers in *Brassica napus* at different developmental stages

Marker type	Tapidor		Ningyou7		Marker number	Subtotal	Methylated alleles (%)	Mapped on LGs	Subtotal	Marker type (%)
	Seedling	Budding	Seedling	Budding						
Stable	−	−	+	+	277	566	86	148	280	90
	+	+	−	−	289			132		
Semistable	+	+	−	+	28	61	9	12	24	8
	−	+	+	+	22			8		
	−	−	+	−	6			1		
	+	−	−	−	5			3		
Unstable	+	−	−	+	14	33	5	2	6	2
	−	+	+	−	19			4		
Total						660			310	

+, methylated alleles; −, unmethylated alleles.

JBnB029F04 was found to contain an identical band as the RTc marker located on linkage group A6. This BAC was used as a probe in BAC–fluorescent *in situ* hybridization (FISH), as described previously (Lim *et al.* 2005).

Analysis of transposon insertion divergence using Hydra

Loci containing structural variants (SVs) between the genomes of TapidorDH and Ningyou7DH were detected using Hydra (Quinlan *et al.* 2010). Solexa GAII paired-end reads (20×) generated from 1-2 kb and 2-3 kb insertion fragments of genomic DNA of Ningyou7DH were mapped to reference sequences of 11 BAC clones of TapidorDH (Cheung *et al.* 2009) available in GenBank. The software Maq (Abbosh *et al.* 2008) was used in the mapping step in place of Burrows-Wheeler Alignment tool (Chinnusamy and Zhu 2009). To identify whether the SV was caused by transposon insertion, SV-containing loci were analyzed using repeatMaster (http://www.repeatmasker.org/cgi-bin/WEBRepeatMasker) with the *Brassica* retrotransposon database (ftp://ftp.tigr.org/pub/data/TransposableElements/transposon_db.pep) and further validated by sequencing the products using the retrotransposon-based insertion polymorphism (RBIP) method (Flavell *et al.* 1998). The SV loci associated with transposon insertion were then mapped to linkage map(s) with the PCR markers.

Results

Epimarkers are stable and informative in B. napus

It was important to establish the stability of specific epimarkers, as by their very nature, modifications such as DNA methylation may give rise to constitutive or dynamic behavior in the context of cell lineages through mitosis, ontogeny, response to environment, or transgenerationally through meiosis. We therefore tested the stability of MSAP markers in different tissues, stages of development, and different environments.

A total of 627 MSAP markers that reported CHG site methylation variation were screened against homozygous parental lines TapidorDH and Ningyou7DH, from leaves 5–6 at seedling stage in autumn (mean 20.7°), and from

buds at floral budding stage in the spring following winter (mean 7.5°), from field-grown plants in Wuhan in the year 2006/2007. A total of 94% of the MSAP markers had a consistent DNA methylation status, of which most (86%) were stable in both parents at both stages/environments. A subset (9%) was stable in only one parent (Table 1). A total of 5% of MSAP markers were variable both between parents and between different developmental stages.

The heritability of DNA methylation patterns was determined in F₁ plants (TapidorDH × Ningyou7DH) with 724 out of 925 (78%) at the seedling stage. A total of 543 (75%) of these loci had identical allelic bands as the dominant allele present in the corresponding parent. Among the dominant loci, the methylated alleles were distributed relatively evenly between the two parents (259:282, χ^2 test, $P > 0.3$).

We checked the stability of MSAP markers in leaves 5–6 from the two parents, and in S5 (self-pollinated fifth generation) lines generated by single-seed descent, grown in the same environment. A total of 36 (97%) of the MSAP markers that were stable between the two developmental stages retained their DNA methylation allelic status through five meioses.

RTg and RTc markers were regarded as stable molecular markers since the assays did not involve the use of methylation sensitive enzymes. The centromeres of 17 linkage groups were identified using 39 RTc markers, with the position of eight centromeres confirmed by both single- and double-insertion RTc markers (Figure 1A; Table S3). The centromeric origin of the marker sequences was confirmed by FISH analysis, using as probes BACs from which the RTc primers had been designed (Figure 1B).

Distribution and density of epiloci within the B. napus genome

We constructed a new linkage map (E-map) with 484 epimarkers and 84 genetic markers. The latter defined the framework in terms of established linkage groups and provided anchors for subsequent comparison with genomic information (Figure 2A; Table S4). A total of 64% (310) of
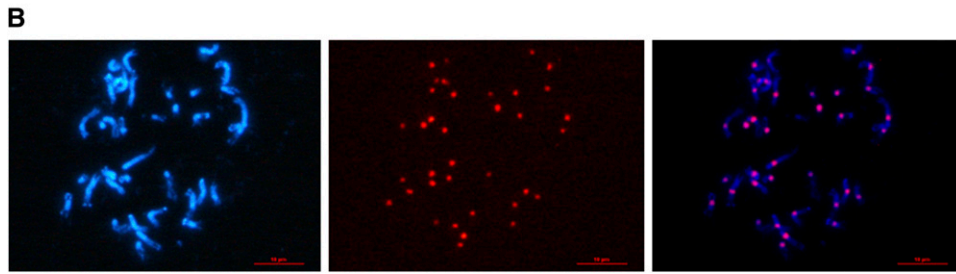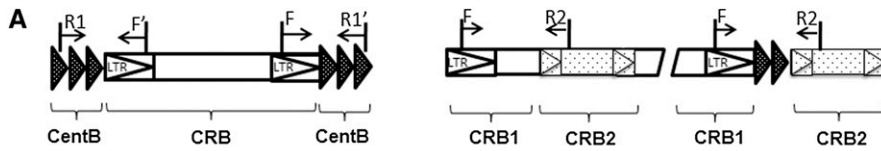
Figure 1 Centromeric retrotransposons (RTc) amplification and confirmation. (A, left) Single insertion of centromeric retrotransposon (CRB) is amplified from within an array of centromere satellite repeats (CentB). (Right) Nested insertion or doubled insertion of retrotransposons is amplified from within an interretrotransposon region, where the PCR products would be expected either to contain CentB in a doubled insertion interretrotransposon or not contain CentB in nested insertion. (B) BAC–FISH analysis using a Tapidor BAC clone (JBnB029F04) containing the RTc sequence used to design primers for the RTc markers. From left to right are chromosomes stained by 4′,6-diamidino-2-phenylindole in blue, FISH signals derived from BAC clone (red), and merged image. A total of 36 of 38 chromosomes with centromeres are visible in the cell. Major signals were localized in the centromere, indicating that the RTc markers were centromere specific.

the 484 MSAP markers placed on the E-map had been confirmed to be consistent either across different developmental stages or environments, and 90% of these (280/310) were stable in both respects (Table 1). Although 36% of mapped MSAP markers were of unknown stability and a few unstable, only those that met the criterion of not influencing the order of non-MSAP genetic markers were retained. This ensured the reliability of the E-map and enabled it to be used for subsequent analysis. Segregation ratios across each chromosome were closely correlated for each type of marker, following similar patterns for the three maps. There appeared to be no bias associated with epimarkers, where 47% had distorted segregation ratios (χ^2 test, $P < 0.05$) compared with 43% for genetic markers, supporting their suitability as reliable genetic markers (Figure 2B). Moreover, there appeared to be no bias introduced into construction of the E-map, with similar numbers of 5mC-derived alleles from each parent line.

The distribution of epiloci appeared to be uneven across the E-map (Figure 2A; Table S5). Analysis with the Poisson distribution function demonstrated that 18% (104) were in clusters of more than eight loci within a 10-cM interval ($P < 0.001$). However, for four epilocus-rich linkage groups (A5, A6, C1, and C4) the clusters were associated with the centromeric region. We identified a larger number of small but distinct clusters that were associated with parent-of-origin DNA methylation, which we termed as E^T cluster (methylated alleles derived from the female TapidorDH parent) and E^N cluster (from Ningyou7DH). A total of 19 $E^{T/N}$ clusters (182 markers) were identified that contained a combination of E^T and E^N methylated alleles within the same region. These were distributed in distinct regions across the genome, covering 16% of the linkage map (296 cM) (Table 2; Figure 2A).

To determine whether this uneven distribution of epiloci was specific to the E-map, the distribution of conventional loci was analyzed within the corresponding BnTNDH G-Map of 648 genetic loci (including the 84 anchoring markers), together with the additional 17 RTc loci (to reveal the position of centromeres) (Table S4). As is common with many genetic maps, there was an uneven distribution of loci in the G-map, with 7 of the 11 clusters identified having a Poisson distribution function located around the centromere.

Since it was difficult to compare the remaining epi- and G-clusters directly, due to lack of common markers within the centromeric regions of the two maps, we generated an integrated map (I-map) using BioMercator 2.0. This consisted of 1157 loci (475 epiloci and 672 genetic loci) covering 2345 cM, with an uneven locus density (Table S4). While there were 1.5 times as many genloci in the A compared with the C genome, there were almost identical numbers of epiloci in each genome. However, the distribution of epiloci on individual linkage groups was extremely uneven, with a notably larger coefficient of variation (0.46) than that of genloci (0.31) (Table 2). A10 had the fewest (4) and lowest density (0.48) of epiloci, while C1 had the most (45) and highest density (7.0), although both linkage groups had a similar number and density of genloci. The I-map retained similar features of cluster distribution for gen- and epiloci as found in the component E- and G-maps (Table S5). Compared with genloci, which were concentrated around the centromeres and formed G-clusters, the epiclusters were distributed throughout the genome. However, there were three overlaps with G-clusters in centromeric regions (Figure 2A). Comparison with the physical map of *B. rapa* chromosome A3 indicated that ~40% of epiloci in *B. napus* linkage group A3 were likely to be located in heterochromatic regions (Figure 2C).

To determine whether the distribution of epiloci was associated with the conserved ancestral blocks arising from sequential ancient duplications within the *Brassicaceae*, we compared homeologous and paralogous regions within the BnTNDH I-map. The 5mC distribution varied among these homologous blocks. For example, the number of epimarkers
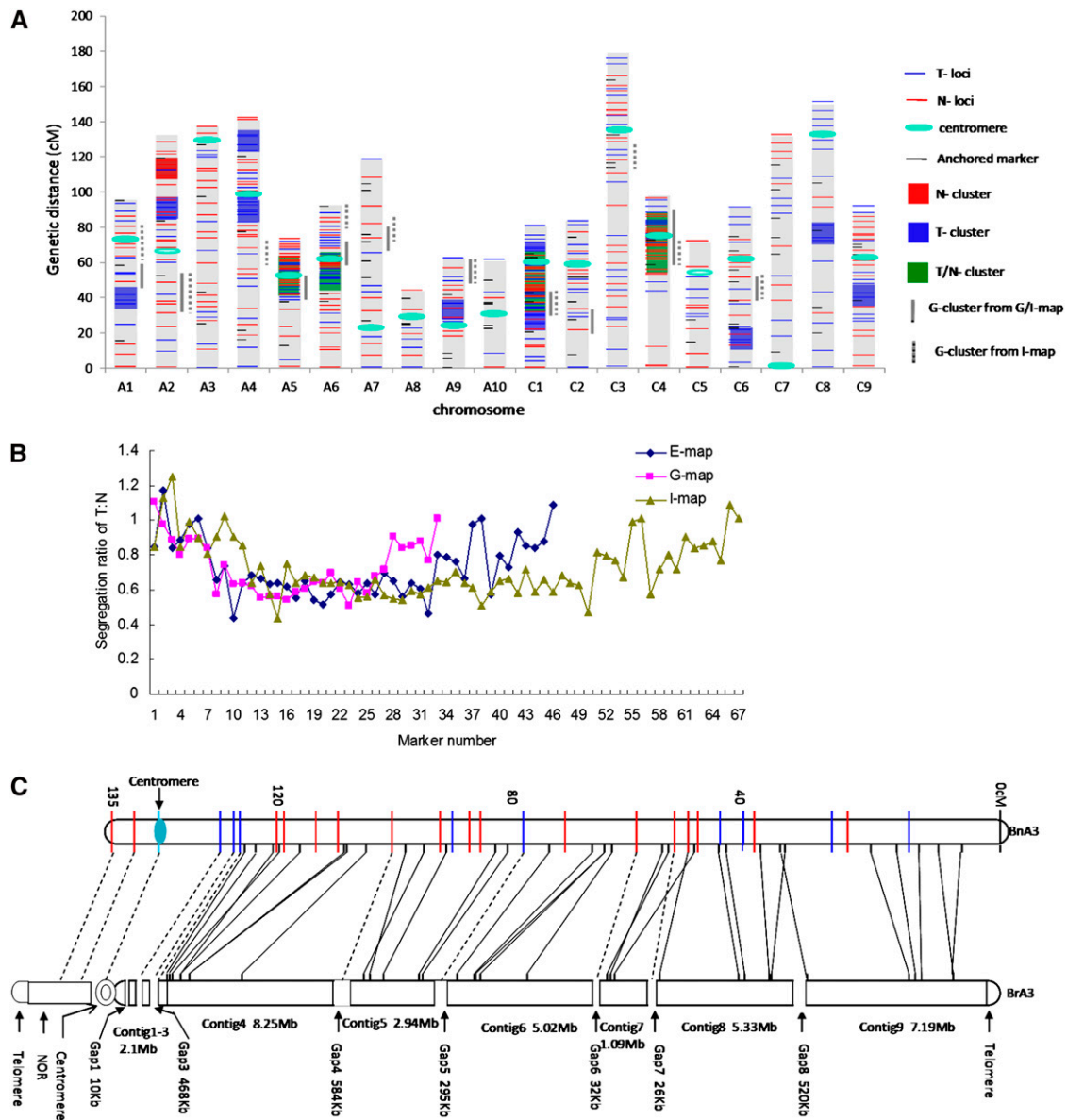
Figure 2 Epilocus distribution and segregation ratio in the map of *Brassica napus*. (A) The landscape of the *B. napus* epigenetic map. Horizontal blue lines represent epialleles from TapidorDH, red lines epialleles from Ningyou7DH, and short black lines represent genmarkers. The red, blue, and green boxes are marker clusters with methylation originating from Ningyou7DH, TapidorDH, or both, respectively. There are 6 N-clusters, 13 T-clusters, and 4 T/N clusters. The vertical gray bars to the right of the LGs indicate genetic-marker clusters, with positions estimated from the common anchored markers in E-map, G-map, and I-map. Centromeres were positioned using RTc markers for 17 of the 19 linkage groups. The locations of the remaining centromeres (in A2 and C5) were estimated by comparison with the corresponding *Arabidopsis* centromere position (Parkin *et al.* 2005). (B) Distribution of parental allelic genotype segregation ratio for the three linkage maps in linkage group C1, which contained the highest number of epimarkers. (C) Comparative mapping of linkage group A3 of *B. napus* (top) and the A3 physical map of *B. rapa* (below, cited from Mun *et al.* 2010). The solid lines between the two maps indicate homologous loci detected by comparative mapping using genetic markers derived from the same *B. rapa* BACs. The dotted lines indicate where epiloci in *B. napus* are likely to correspond to heterochromatic regions (NOR, centromere and gaps that remained un-assembled due to prevalence of repeat sequences) of the *B. rapa* A3 chromosome.

in block U (*sensu* Schranz) varied considerably within the four linkage groups A1 (15), A3 (4), A8 (4), and C7 (7).

DNA sequence properties associated with epiloci

We sequenced MSAP bands associated with 15 epiloci distributed across 10 linkage groups and found that about half of these were from genes coding for various proteins (8 sequences) or putative regulatory sequence (3 sequences) as identified by motif prediction. Most of the remaining sequences (5/15) were retrotransposon related (Figure S1A; Table S6). We confirmed that all 15 MSAP bands contained the methylation sensitive restriction cutting site CTGCAG.

Both RTg markers were sequenced and found to possess the LTR of the retrotransposon that had been used in the primer design, as well as a flanking sequence falling within a genic region, indicating that this type of marker was reliable

Table 2 Number of epi- and genmarkers and clusters identified within the TNDH I-map

| LG | Number of markers | | | Cluster | LG | Number of markers | | | Cluster |
| | Epi- | Gen- | Total | | | Epi- | Gen- | Total | |
	A genome					C genome			
A1	23	44	67	G-cluster (1)[a]	C1	45	25	70	E-cluster (3) G-cluster (1)
A2	35	29	64	—	C2	20	25	45	—
A3	27	36	97	G-cluster (1)	C3	36	49	85	G-cluster (1)
A4	37	27	64	E-cluster (2)	C4	40	32	72	E-cluster (2) G-cluster (1)
A5	29	41	70	G-cluster (1)	C5	12	19	31	—
A6	40	51	91	E-cluster (2) G-cluster (1)	C6	22	31	53	G-cluster (1)
A7	16	46	62	G-cluster (1)	C7	16	22	38	—
A8	9	27	36	G-cluster (1)	C8	19	20	39	—
A9	18	36	88	G-cluster (1)	C9	27	23	50	—
A10	4	31	35	—					
Subtotal	238	368	674	11	Subtotal	237	246	483	9
CV	0.46				CV	0.31			

CV, coefficient of variation.

[a] Numbers in parentheses indicates the number of clusters detected in each linkage group.

(Figure S1B). Sequence analysis following cloning of 10 RTc markers confirmed that these were related to known centromere retrotransposons, and all sequences had high identity with the centromere-specific retrotransposon in the original *B. rapa* BAC (Lim *et al.* 2007). Three subclasses of centromeric sequences were detected, all possessing centromere retrotransposon LTR sequences, thus confirming that the RTc loci are most likely to be an accurate representation of the centromeric region (Figure S1C). As expected, the polymorphism of RTc markers arose from retrotransposon insertion–deletion events in the centromere region.

We analyzed sequence structural variation between the two parents using Hydra for a 1.8-Mb BAC sequence of TapidorDH (covering 0.7% of the genome) and 1.25 million Solexa reads of Ningyou7DH. A total of 18 structural variants were identified, of which half represented insertions and half represented deletions in Ningyou7DH. Of the nine deletion loci in Ningyou7DH, seven were possibly related to transposon insertion events in TapidorDH. Three of the events were validated by PCR amplification (Figure S1D), and found to be caused by transposon insertion into the TapidorDH genome, mapping to linkage groups A1, A3, and C9.

Detection and features of QTL^epi

QTL controlling seven different traits, evaluated in 2–10 different environments, were identified and assigned as QTL^epi or QTL^dna, dependent upon their detection in either the E-map or G-map, respectively. Within the context of the I-map, where the confidence interval was solely associated with one class of locus, the QTL were further assigned as QTL^epi-c (confident for QTL^epi) and QTL^dna-c (confident for QTL^dna), respectively. Conversely, where the confidence interval was associated with a combination of epi- and genloci, the QTL was assigned as QTL^epi-l (QTL^epi-like) or QTL^dna-l (QTL^dna-like) according to whether the QTL peak position was closer to the epilocus or genlocus, respectively. For some traits, the same QTL positions could be identified from multiple environments, and these were assigned as "recurring" QTL and integrated into consensus QTL by meta-analysis to avoid overestimating the number. A total of 125 consensus QTL^epi were detected from the E-map for the seven traits, compared with 148 (92%) QTL^dna detected from the G-map (Table S7). A total of 26% of the QTL^epi were distributed in epicluster regions, twice the average (1 QTL^epi/17 cM) (χ^2 test, $P < 0.01$). None of the six unstable markers were located within the confidence intervals of QTL^epi in either the E-map or I-map.

Although fewer QTL^epi were detected in the I-map compared with the E-map, these still accounted for 28% of the total detected QTL, with 72% of QTL^epi distributed on just nine linkage groups. Three linkage groups (A4, A6, and C8) contained more QTL^epi than QTL^dna (Table S8; Figure 3A). Conversely, only a few QTL^epi were detected on linkage groups A10 and C7, with a very low QTL density in the latter. Linkage group C4 had both the lowest number and density of QTL at both epigenetic and genetic levels.

We tested the hypothesis of an interaction between QTL^epi and environmental specificity. As expected, the number of QTL detected increased with the number of environments, with some QTL being specific to particular environments. Three parameters were calculated for each trait: the average number of QTL identified from one environment; the total integrated consensus QTL detected from all environments; and the index of environmental specificity, which we define as the ratio of consensus QTL to primary QTL for each trait (Table S9). In general, the average number of primary QTL^epi detected from one environment was half that of QTL^dna (18.3 *vs.* 39.5). Thus it appears there are no substantial differences between QTL^epi and QTL^dna in terms of the index of environmental specificity when the
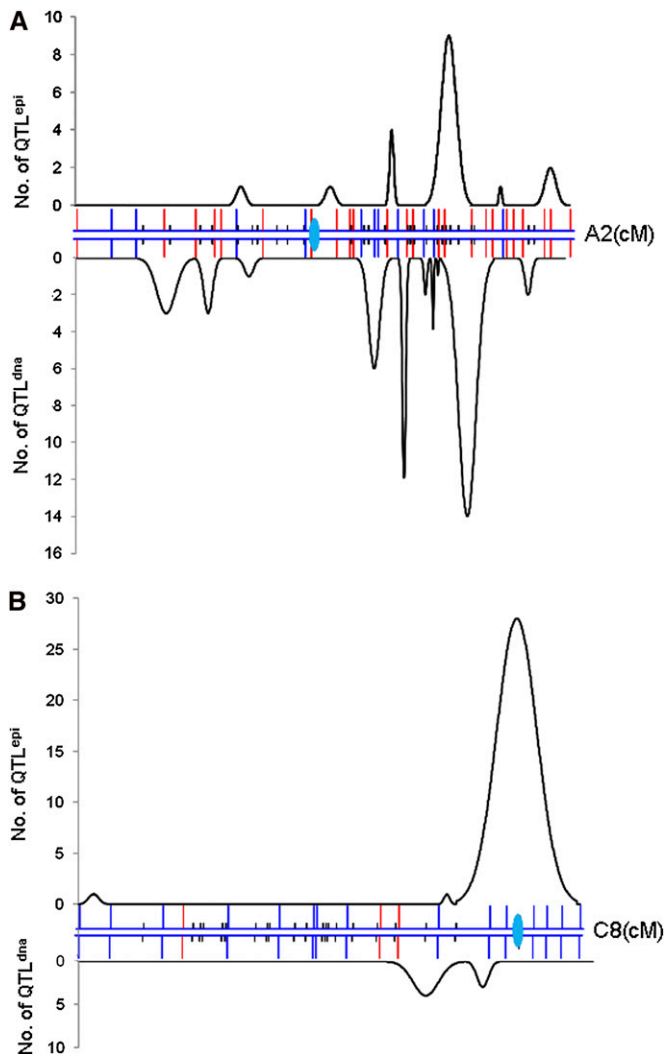
Figure 3 Distribution of consensus QTL^{epi} on the I-map linkage groups. (A) Distribution of QTL^{epi} and QTL^{dna} on linkage group A2. (B) Distribution of QTL^{epi} and QTL^{dna} on linkage group C8. The curves above and below the LG represent QTL^{epi} and QTL^{dna}, regardless of LOD value, and take into account solely the number of QTL. The height of the curve represents the frequency of QTL detected, and the width of the baseline of the curve represents the extent of confidence intervals for the QTL in that region.

combined sets of four types of traits are taken into consideration.

Discussion

We have characterized the inheritance and distribution of two classes of epimarker within the complex *B. napus* genome. We found 90% of mapped epimarkers retained the same pattern in two contrasting developmental stages and environments. For two distinct parental lines, 97% of alleles were transmitted through five meioses. Epimarkers were distributed nonrandomly in the genome and appeared to affect the ability to detect recombination. A total of 125 QTL were associated with seven agronomic traits in regions having a greater density of DNA methylation markers. Our

results will not only facilitate further characterization of epiloci, but also assist assembly of the complex *B. napus* polyploid genome, currently being sequenced using high throughput sequencing technology.

The centromere is a heterochromatic region where transposons accumulate, with consequent high levels of DNA methylation (Zilberman *et al.* 2007). Accurate mapping of centromeres is an important step for genomic and epigenomic studies. Although Pouilly *et al.* (2008) mapped centromere-related transposons on *B. napus* linkage maps, the definitive centromere position in each linkage group has been uncertain. Our accurate mapping of 17 of 19 centromeres with centromere-specific markers was confirmed by BAC–FISH and a published physical sequence map (A3).

Functional genes have recently been identified within centromeric regions of plants such as rice and wheat (Nagaki *et al.* 2004; Mutti *et al.* 2010). Interestingly, we found that the increased map resolution afforded by centromeric and epimarkers enabled us to detect a significant number of QTL^{epi} (14% of total) associated with seven traits in the centromeric regions of five linkage groups. Recombination has been shown in genetic and cytological studies to be severely suppressed in plant centromeric regions (Ma *et al.* 2007), with reduced recombination frequency detected by conventional markers. Using chromosome orientation FISH (CO-FISH), Jaco *et al.* (2008) found high mitotic recombination frequency at mouse centromeres and established that DNA methylation was a negative regulator of centromere recombination. Our results suggest epimarkers may provide complementary information to reassess recombination frequency in centromeric regions.

We have demonstrated that most MSAP markers are transgenerationally stable through five successive meioses for the parent lines, and that polymorphic MSAP alleles still segregate in a Mendelian fashion in the BnTNDH population after three meioses following original fixation by microspore culture. DNA methylation was relatively stable at polymorphic loci. Only 5% of 627 MSAP markers were variable at different developmental stages following growth in contrasting environments. Only 6% of mapped MSAP markers were unstable. In plants, patterns of DNA methylation can be faithfully maintained across generations and transmitted through mitosis and/or meiosis (Martienssen and Colot 2001; Saze 2008). Hypomethylated *Arabidopsis* epi-recombinant inbred lines have been established varying with high heritability for flowering time and plant height, and stable inheritance of multiple parental DNA methylation variants over at least eight generations (Johannes *et al.* 2008).

Overall, there was a similar number of epialleles in each of the two parental genomes. However, more were detected in the A genome for Ningyou7DH (127) than TapidorDH (100), with identical numbers (114) in the C genome. We found 1.5 times more informative genmarkers within the A genome compared with the C. This may reflect the breeding pedigree of the Ningyou7DH parents, where *B. rapa* (AA)

contributed as a recent ancestor, and *de novo* DNA methylation may have arisen during introgression to the A genome of *B. napus*. Hybrids from interspecific crosses in *Arabidopsis* (Bushell *et al.* 2003) and cotton (Keyte *et al.* 2006) show changes in the DNA methylation pattern compared with parents, and *de novo* methylation and demethylation occur in interspecific hybrids of beans (Abid *et al.* 2011).

Epiloci were unevenly distributed between linkage groups, with C1 having the greatest number (45) and density (7.0 per 10 cM), >10 times that within A10. This pattern of differential methylation was also detected between homologous ancestral blocks and may reflect a buffer of gene dosage resulting from formation of the amphidiploid (Paun *et al.* 2010). In primate genomes, the degree of CpG methylation in homologous genomic regions varies between human, chimpanzee and baboon (Meunier *et al.* 2005), suggesting the existence of a homology-dependent methylation (HDM) mechanism.

The uneven distribution of epiloci between the A and C genomes, between chromosomes and homologous blocks, may indicate that genome evolution of *B. napus* has directly or indirectly involved activation or repression of transposons during speciation, cultivar breeding, and possibly arising from cultivation in different environments, which in turn may contribute to the adaptation of different cultivars (Feinberg and Irizarry 2010; Yi *et al.* 2010)

Conventional QTL analysis relies on detection of recombination using DNA markers where parental alleles cosegregate with heritable phenotypic variation. These have been referred to as QTL[dna] to distinguish from QTL[epi], resolved by detection of recombination using a DNA methylation polymorphism within the corresponding genomic region (Johannes *et al.* 2008). We used MSAP and retrotransposon-specific markers to reveal QTL[epi], where the parental epialleles cosegregate with a trait in the BnTNDH population.

The epimarkers detected additional chiasmata within the population. We took care to ensure that the pattern of segregation and detection of chiasmata was consistent with the conventional genmarkers within each linkage group. The congruent pattern of segregation distortion for epi- and genmarkers along each chromosome also gave us confidence that the epimarkers provide an accurate reflection of recombination within the population. This has consequences for understanding the distribution of recombination frequency in different populations for the ability to detect and resolve QTL and for map-based cloning.

For seven traits in multiple environments, we detected between 2 and 17 QTL[epi] each, depending on the trait *per se* and the number of environments in which different traits were scored. The increased ability to resolve previously "cryptic" QTL suggests that studies relying solely on polymorphism of conventional genmarkers may consistently underestimate the quantity and distribution of QTL effects. We found that QTL[epi] were unevenly distributed among chromosomes, with 8 (12%) on C8 controlling plant develop-

ment and one seed quality trait, while only 4 (2%) QTL[dna] were detected on the same chromosome. This suggests that human selection may have a strong impact on specific chromosomes, where the activities of transposons affect agronomic traits, as indicated by Hauben *et al.* (2009) in *B. napus*. Within chromosome C4, which contained more epiloci (39) than genloci (32), only 2 QTL[dna] and no QTL[epi] were detected. This chromosome may possess more heterochromatin and/or functional genes in regions of reduced polymorphism. Further interpretation of the QTL[epi] requires establishing a direct causality between the epigenetic status of any functional genes and the trait controlled by the QTL[epi].

Retrotransposons have been estimated by FISH and sequence analysis to represent ∼30% of the *B. rapa* A genome (Lim *et al.* 2005; Hong *et al.* 2006). We found a similar proportion in *B. napus*, on the basis of BAC end sequence analysis (our unpublished data). This major contribution of transposable elements may provide genomic loci for epimarkers that then enable detection of additional QTL. Moreover, these QTL[epi] had equally as strong environment interaction as those of QTL[dna] (Table S9). Artificial reduction of DNA methylation has demonstrated effects on a wide range of phenotypic traits (King 1995; Finnegan *et al.* 1998; Johannes *et al.* 2008). Our results suggest that naturally occurring variation associated with DNA methylation may also generate epiallelic variation, able to be detected as marker polymorphism in regions where conventional genetic markers are monomorphic. Similar conclusions have been reached by recent selection studies in *Brassica* by Hauben *et al.* (2009) and Ni *et al.* (2009).

Acknowledgments

Literature Cited

Abbosh, P. H., M. Wang, J. N. Eble, A. Lopez-Beltran, G. T. Maclennan *et al.*, 2008 Hypermethylation of tumor-suppressor gene CpG islands in small-cell carcinoma of the urinary bladder. Mod. Pathol. 21: 355–362.

Abid, G., Y. Muhoviski, J. M. Jacquemin, D. Mingeot, K. Sassi *et al.*, 2011 Changes in DNA-methylation during zygotic embryogenesis in interspecific hybrids of beans (Phaseolus ssp.). Plant Cell Tissue Organ Cult. 105: 383–393.

Allender, C. J., and G. J. King, 2010 Origins of the amphiploid species Brassica napus L. investigated by chloroplast and nuclear molecular markers. BMC Plant Biol. 10: 54.

Braszewska-Zalewska, A., T. Bernas, and J. Maluszynska, 2010 Epigenetic chromatin modifications in *Brassica* genomes. Genome 53: 203–210.

Bushell, C., M. Spielman, and R. J. Scott, 2003 The basis of natural and artificial postzygotic hybridization barriers in *Arabidopsis* species. Plant Cell 15: 1430–1442.

Cheung, F., M. Trick, N. Drou, Y. P. Lim, J. Y. Park et al., 2009 Comparative analysis between because genome segments of *Brassica napus* and its progenitor species reveals extensive sequence-level divergence. Plant Cell 21: 1912–1928.

Chinnusamy, V., and J. K. Zhu, 2009 Epigenetic regulation of stress responses in plants. Curr. Opin. Plant Biol. 12: 133–139.

Churchill, G. A., and R. W. Doerge, 1994 Empirical threshold values for quantitative trait mapping. Genetics 138: 963–971.

Ellis, T. H., S. J. Poyser, M. R. Knox, A. V. Vershinin, and M. J. Ambrose, 1998 Polymorphism of insertion sites of Ty1-copia class retrotransposons and its use for linkage and diversity analysis in pea. Mol. Gen. Genet. 260: 9–19.

Feinberg, A. P., and R. A. Irizarry, 2010 Stochastic epigenetic variation as a driving force of development, evolutionary adaptation, and disease. Proc. Natl. Acad. Sci. USA 107: 1757–1764.

Finnegan, E. J., R. K. Genger, W. J. Peacock, and E. S. Dennis, 1998 DNA methylation in plants. Annu. Rev. Plant Physiol. Plant Mol. Biol. 49: 223–247.

Finnegan, E. J., W. J. Peacock, and E. S. Dennis, 2000 DNA methylation, a key regulator of plant development and other processes. Curr. Opin. Genet. Dev. 10: 217–223.

Flavell, A. J., M. R. Knox, S. R. Pearce, and T. H. Ellis, 1998 Retrotransposon-based insertion polymorphisms (RBIP) for high throughput marker analysis. Plant J. 16: 643–650.

Gehring, M., K. L. Bubb, and S. Henikoff, 2009 Extensive demethylation of repetitive elements during seed development underlies gene imprinting. Science 324: 1447–1451.

Gruenbaum, Y., T. Naveh-Many, H. Cedar, and A. Razin, 1981 Sequence specificity of methylation in higher plant DNA. Nature 292: 860–862.

Han, Y., G. Wang, Z. Liu, J. Liu, W. Yue et al., 2010 Divergence in centromere structure distinguishes related genomes in *Coix lacryma-jobi* and its wild relative. Chromosoma 119: 89–98.

Hauben, M., B. Haesendonckx, E. Standaert, K. Van Der Kelen, A. Azmi et al., 2009 Energy use efficiency is characterized by an epigenetic component that can be directed through artificial selection to increase yield. Proc. Natl. Acad. Sci. USA 106: 20109–20114.

Hong, C. P., P. Plaha, D. H. Koo, T. J. Yang, S. R. Choi et al., 2006 A survey of the *Brassica rapa* genome by BAC-end sequence analysis and comparison with *Arabidopsis thaliana*. Mol. Cells 22: 300–307.

Horváth, E., G. Szalai, T. Janda, E. Páldi, I. Rácz et al., 2002 Effect of vernalisation and azacytidine on the DNA methylation. Acta Biologica Szegediensis 46: 35–36.

Inaba, R., and T. Nishio, 2002 Phylogenetic analysis of *Brassiceae* based on the nucleotide sequences of the *S*-locus related gene, *SLR1*. Theor. Appl. Genet. 105: 1159–1165.

Jaco, I., A. Canela, E. Vera, and M. A. Blasco, 2008 Centromere mitotic recombination in mammalian cells. J. Cell Biol. 181: 885–892.

Johannes, F., V. Colot, and R. C. Jansen, 2008 Epigenome dynamics: a quantitative genetics perspective. Nat. Rev. Genet. 9: 883–890.

Johnston, J. S., A. E. Pepper, A. E. Hall, Z. J. Chen, G. Hodnett et al., 2005 Evolution of genome size in *Brassicaceae*. Ann. Bot. (Lond.) 95: 229–235.

Kakutani, T., K. Munakata, E. J. Richards, and H. Hirochika, 1999 Meiotically and mitotically stable inheritance of DNA hypomethylation induced by *ddm1* mutation of *Arabidopsis thaliana*. Genetics 151: 831–838.

Kalisz, S., and M. D. Purugganan, 2004 Epialleles via DNA methylation: consequences for plant evolution. Trends Ecol. Evol. 19: 309–314.

Keyte, A. L., R. Percifield, B. Liu, and J. F. Wendel, 2006 Infraspecific DNA methylation polymorphism in cotton (*Gossypium hirsutum* L.). J. Hered. 97: 444–450.

King, G. J., 1995 Morphological development in brassica-oleracea is modulated by in-vivo treatment with 5-azacytidine. J. Hortic. Sci. 70: 333–342.

King, G. J., S. Amoah, and S. Kurup, 2010 Exploring and exploiting epigenetic variation in crops. Genome 53: 856–868.

Kondo, H., H. Ozaki, K. Itoh, A. Kato, and K. Takeno, 2006 Flowering induced by 5-azacytidine, a DNA demethylating reagent in a short-day plant, *Perilla frutescens* var. *crispa*. Physiol. Plant. 127: 130–137.

Kovarik, A., R. Matyasek, A. Leitch, B. Gazdova, J. Fulnecek et al., 1997 Variability in CpNpG methylation in higher plant genomes. Gene 204: 25–33.

Kwon, S. J., D. H. Kim, M. H. Lim, Y. Long, J. L. Meng et al., 2007 Terminal repeat retrotransposon in miniature (TRIM) as DNA markers in *Brassica* relatives. Mol. Genet. Genomics 278: 361–370.

Lim, K. B., H. de Jong, T. J. Yang, J. Y. Park, S. J. Kwon et al., 2005 Characterization of rDNAs and tandem repeats in the heterochromatin of *Brassica rapa*. Mol. Cells 19: 436–444.

Lim, K. B., T. J. Yang, Y. J. Hwang, J. S. Kim, J. Y. Park et al., 2007 Characterization of the centromere and peri-centromere retrotransposons in *Brassica rapa* and their distribution in related *Brassica* species. Plant J. 49: 173–183.

Lister, R., R. C. O'Malley, J. Tonti-Filippini, B. D. Gregory, C. C. Berry et al., 2008 Highly integrated single-base resolution maps of the epigenome in *Arabidopsis*. Cell 133: 523–536.

Long, Y., J. Shi, D. Qiu, R. Li, C. Zhang et al., 2007 Flowering time quantitative trait loci analysis of oilseed *Brassica* in multiple environments and genomewide alignment with *Arabidopsis*. Genetics 177: 2433–2444.

Ma, J., R. A. Wing, J. L. Bennetzen, and S. A. Jackson, 2007 Plant centromere organization: a dynamic structure with conserved functions. Trends Genet. 23: 134–139.

Manning, K., M. Tor, M. Poole, Y. Hong, A. J. Thompson et al., 2006 A naturally occurring epigenetic mutation in a gene encoding an SBP-box transcription factor inhibits tomato fruit ripening. Nat. Genet. 38: 948–952.

Martienssen, R. A., and V. Colot, 2001 DNA methylation and epigenetic inheritance in plants and filamentous fungi. Science 293: 1070–1074.

Messeguer, R., M. W. Ganal, J. C. Steffens, and S. D. Tanksley, 1991 Characterization of the level, target sites and inheritance of cytosine methylation in tomato nuclear DNA. Plant Mol. Biol. 16: 753–770.

Meunier, J., A. Khelifi, V. Navratil, and L. Duret, 2005 Homology-dependent methylation in primate repetitive DNA. Proc. Natl. Acad. Sci. USA 102: 5471–5476.

Mun, J. H., S. J. Kwon, Y. J. Seol, J. A. Kim, M. Jin et al., 2010 Sequence and structure of *Brassica rapa* chromosome A3. Genome Biol. 11: R94.

Mutti, J. S., D. Sandhu, D. Sidhu, and K. S. Gill, 2010 Dynamic nature of a wheat centromere with a functional gene. Mol. Breed. 26: 177–187.

Nagaki, K., Z. Cheng, S. Ouyang, P. B. Talbert, M. Kim et al., 2004 Sequencing of a rice centromere uncovers active genes. Nat. Genet. 36: 138–145.

Ni, Z., E. D. Kim, M. Ha, E. Lackey, J. Liu et al., 2009 Altered circadian rhythms regulate growth vigour in hybrids and allopolyploids. Nature 457: 327–331.

Papa, C. M., N. M. Springer, M. G. Muszynski, R. Meeley, and S. M. Kaeppler, 2001 Maize chromomethylase Zea *methyltransferase2* is required for CpNpG methylation. Plant Cell 13: 1919–1928.

Parkin, I. A., S. M. Gulden, A. G. Sharpe, L. Lukens, M. Trick et al., 2005 Segmental structure of the *Brassica napus* genome based on comparative analysis with *Arabidopsis thaliana*. Genetics 171: 765–781.

Paun, O., R. M. Bateman, M. F. Fay, M. Hedren, L. Civeyrel *et al.*, 2010 Stable epigenetic effects impact adaptation in allopolyploid orchids (*Dactylorhiza*: Orchidaceae). Mol. Biol. Evol. 27: 2465–2473.

Pouilly, N., R. Delourme, K. Alix, and E. Jenczewski, 2008 Repetitive sequence-derived markers tag centromeres and telomeres and provide insights into chromosome evolution in *Brassica napus*. Chrom. Res. 16: 683–700.

Prieto, J. L., N. Pouilly, E. Jenczewski, J. M. Deragon, and A. M. Chevre, 2005 Development of crop-specific transposable element (SINE) markers for studying gene flow from oilseed rape to wild radish. Theor. Appl. Genet. 111: 446–455.

Qiu, D., C. Morgan, J. Shi, Y. Long, J. Liu *et al.*, 2006 A comparative linkage map of oilseed rape and its use for QTL analysis of seed oil and erucic acid content. Theor. Appl. Genet. 114: 67–80.

Quinlan, A. R., R. A. Clark, S. Sokolova, M. L. Leibowitz, Y. Zhang *et al.*, 2010 Genome-wide mapping and assembly of structural variant breakpoints in the mouse genome. Genome Res. 20: 623–635.

Reyna-Lopez, G. E., J. Simpson, and J. Ruiz-Herrera, 1997 Differences in DNA methylation patterns are detectable during the dimorphic transition of fungi by amplification of restriction polymorphisms. Mol. Gen. Genet. 253: 703–710.

Robertson, K. D., 2005 DNA methylation and human disease. Nat. Rev. Genet. 6: 597–610.

Salmon, A., J. Clotault, E. Jenczewski, V. Chable, and M. J. Manzanares-Dauleux, 2008 *Brassica oleracea* displays a high level of DNA methylation polymorphism. Plant Sci. 174: 61–70.

Saze, H., 2008 Epigenetic memory transmission through mitosis and meiosis in plants. Semin. Cell Dev. Biol. 19: 527–536.

Shi, J., R. Li, D. Qiu, C. Jiang, Y. Long *et al.*, 2009 Unraveling the complex trait of crop yield with quantitative trait loci mapping in *Brassica napus*. Genetics 182: 851–861.

Shiba, H., T. Kakizaki, M. Iwano, Y. Tarutani, M. Watanabe *et al.*, 2006 Dominance relationships between self-incompatibility alleles controlled by DNA methylation. Nat. Genet. 38: 297–299.

Slotkin, R. K., and R. Martienssen, 2007 Transposable elements and the epigenetic regulation of the genome. Nat. Rev. Genet. 8: 272–285.

Suzuki, M. M., and A. Bird, 2008 DNA methylation landscapes: provocative insights from epigenomics. Nat. Rev. Genet. 9: 465–476.

Van Ooijen, J. W., 2006 *JoinMap4, software for the calculation of genetic linkage maps in experimental populations*. Kyazma B. V., Wageningen, The Netherlands.

Vuylsteke, M., R. Mank, R. Antonise, E. Bastiaans, M. L. Senior *et al.*, 1999 Two high-density AFLP linkage maps of Zea mays L.: analysis of distribution of AFLP markers. Theor. Appl. Genet. 99: 921–935.

Wang, S. C., J. Bastern, and Z. B. Zeng, 2006 Windows QTL Cartographer 2.5. Department of Statistics, North Carolina State University, Raleigh, NC. (http://statgen.ncsu.edu/qtlcart/WQTLCart.htm).

Watanabe, Y., and M. Maekawa, 2010 Methylation of DNA in cancer. Adv. Clin. Chem. 52: 145–167.

Waugh, R., K. McLean, A. J. Flavell, S. R. Pearce, A. Kumar *et al.*, 1997 Genetic distribution of Bare-1-like retrotransposable elements in the barley genome revealed by sequence-specific amplification polymorphisms (S-SAP). Mol. Gen. Genet. 253: 687–694.

Yan, H., S. Kikuchi, P. Neumann, W. Zhang, Y. Wu *et al.*, 2010 Genome-wide mapping of cytosine methylation revealed dynamic DNA methylation patterns associated with genes and centromeres in rice. Plant J. 63: 353–365.

Yang, T.-J., J. S. Kim, S.-J. Kwon, K.-B. Lim, B.-S. Choi *et al.*, 2006 Sequence-level analysis of the diploidization process in the triplicated *FLOWERING LOCUS C* region of *Brassica rapa*. Plant Cell 18: 1339–1347.

Yi, C. X., S. L. Zhang, X. K. Liu, H. T. N. Bui, and Y. Hong, 2010 Does epigenetic polymorphism contribute to phenotypic variances in *Jatropha curcas* L.? BMC Plant Biol. 10: 259.

Zilberman, D., M. Gehring, R. K. Tran, T. Ballinger, and S. Henikoff, 2007 Genome-wide analysis of *Arabidopsis thaliana* DNA methylation uncovers an interdependence between methylation and transcription. Nat. Genet. 39: 61–69.

Communicating editor: Andrew H. Paterson

GENETICS

Epigenetic QTL Mapping in *Brassica napus*

Yan Long, Wei Xia, Ruiyuan Li, Jing Wang, Mingqin Shao, Ji Feng, Graham J. King, and Jinling Meng
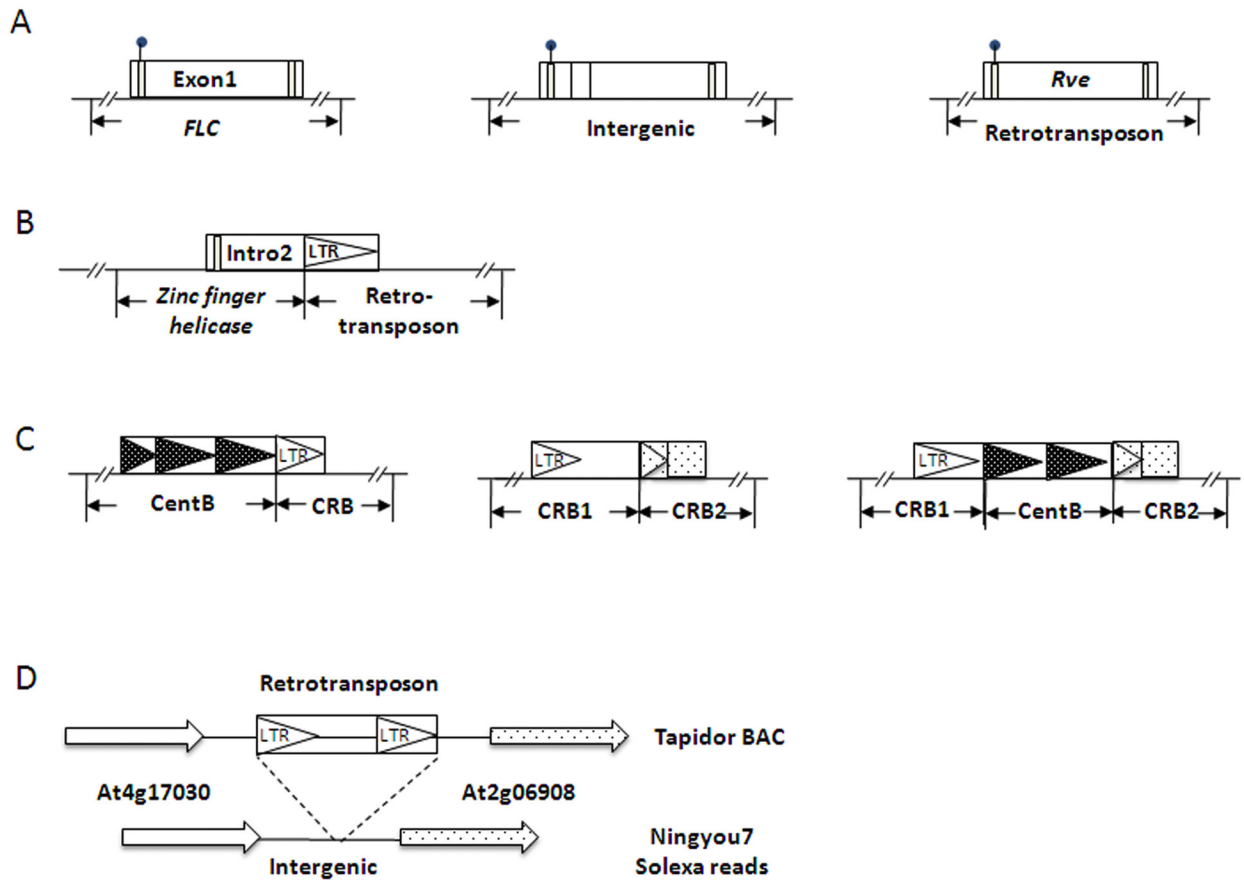
Figure S1 Characterizing DNA sequences from Epi-loci. The cloned sequence is represented by a rectangle above the line in A-C. (A) Three types of MSAP fragment containing coding sequence (left), intergenic region with motif (GT-3a box III shown with yellow box, middle) and retrotransposon (right). The restriction site is indicated by grey box B, and the methylation site indicated by a black dot. (B) A RTg marker sequnce containing fragments of zinc finger helicase (At2g47680) and retrotransposon. (C) A single retrotransposon insertion (left) and double retrotransposon insertion (middle and right) were detected from RTc markers. (D) Transposon insertion in TapidorDH (detected from BAC accession AC236786) caused a structural variation compared to Ningyou7DH.

Table S1   List of sixteen agronomic traits from two to ten environments

Table S2   Primer information of MSAP and retrotransposon sprcific markers

Tables S1 and S2 are available for download as Excel files at
http://www.genetics.org/content/suppl/2011/09/02/genetics.111.131615.DC1.

Table S3   Information of RTc Primer pairs and the amplified markers in I-map

Chromosome	No. of T dominant marker	No. of N dominant marker	Total	position	No. of single insertion RTc markers	No. of double insertion RTc markers
A1	2	0	2	74.4	0	2
A2	0	0	0	-	0	0
A3	1	0	1	128.3	0	1
A4	2	0	2	81.7	1	1
A5	1	2	3	61.1	1	2
A6	5	3	8	95.3	2	6
A7	0	3	3	30.4	1	2
A8	1	0	1	75.3	1	0
A9	2	2	4	75.1	3	1
A10	1	1	2	7.1	1	1
C1	1	1	2	54	1	1
C2	1	0	1	77.9	0	1
C3	1	1	2	113.7	0	2
C4	1	1	2	66.2	0	2
C5	0	0	0	-	0	0
C6	1	1	2	85	0	2
C7	1	0	1	0	0	1
C8	1	0	1	114.8	1	0
C9	2	0	2	77.6	1	1
Total	24	15	39		13	26

Table S4   E-map, G-map, and I-map and genotype

Table S4 is available for download a compressed Excel file at
http://www.genetics.org/content/suppl/2011/09/02/genetics.111.131615.DC1.

Table S5   Genetic position of three type of clusters

	E-map					G-map			I-map
	T-cluster	N-cluster	Total	NO T/N	G-cluster	T-cluster	N-cluster	Total	G-cluster
LG	(cM)	(cM)	(cM)	(cM)	(cM)	(cM)	(cM)	(cM)	(cM)
A1	34-52	-	34-52	-	50-60	-	-	-	60-80
A2	87-97	109-119	87-97/109-119	-	-	-	-	-	-
A3	-	-	-	-	30-50	-	-	-	30-50
A4	83-93/123-133	-	83-93/123-133	-	-	71-81	69-79	70-80	-
A5	32-52	45-76	32-52/45-76	40-70	50-60	-	-	-	60-70
A6	38-73	28-38/45-64	28-38/38-73	40-70	60-70	-	64-74/89-99	64-74/89-99	80-90
A7	-	-	-	-	70-80	-	-	-	75-85
A8	-	-	-	-	60-70	-	-	-	61-71
A9	24-34	-	24-34	-	70-80	-	-	-	70-80
A10	-	-	-	-	-	-	-	-	-
C1	21-41/51-73	35-55	21-41/51-73	30-60	30-40	20-30/44-66	20-50	20-66	30-40
C2	-	-	-	-	-	-	-	-	-
C3	-	-	-	-	20-30	-	-	-	110-120
C4	80-90	55-85	55-90	60-90	60-70	72-82	48-78	48-82	60-70
C5	-	-	-	-	-	-	-	-	-
C6	14-24	-	14-24	-	40-50	-	-	-	40-50
C7	-	-	-	-	-	-	-	-	-
C8	71-81	-	71-81	-	-	-	-	-	-
C9	38-48	-	38-48	-	-	-	-	-	-

Table S6 List of allelic sequence information of epi-loci

Marker type	Marker name	Linkage group	Marker position on I-map	Sequence information for the allele of Tapidor	Sequence information for the allele of Ningyou7
	P04M04-300-N	A01	34.1	No methylation	Hypothetical protein
	P06M03-240-T	A01	50	Copia-like polyprotein	No methylation
	P04M04-370-N	A01	77.7	No methylation	Putative non-LTR reverse transcriptase
	P08M03-295-T	A02	104.9	Hypothetical protein ARALYDRAFT_488148	No methylation
	P08M01-160-N	A02	108.8	No methylation	Putative non-LTR retroelement reverse transcriptase
	P01M09-140-N	A02	115.6	No methylation	Contain motif GT-3a Box III (ACtGTTACACT, DNA binding factor):
	P04M02-260-N	A02	81.9	No methylation	Putative cell division membrane protein
	P13M16-350-N	A03	47.7	No methylation	Brassica oleracea var. alboglabra flc3 gene for flowering protein
	P01M09-350-N	A06	16.3		Retroelement pol polyprotein-like
	P08M01-90-N	C01	39.8	No methylation	Contain 3 motifs: VP1(CGTaCATGCAg,); C-box(ATGAGTCcT); GA-5(AGAGAGAcA). DNA binding factor
	P10M08-150-N	C03	128	No methylation	Contain 3 motifs:S1(GATTCCATG); GT-1-like K(AGGCATT); B5(GTTGACCTGA). Regulatory elements
	P08M24-140-N	C03	146.7	No methylation	Oxysterol-binding family protein
	P02M10-305-N	C04	70.4	No methylation	Copia-type polyprotein
	P08M24-460-N	C07	29.8	No methylation	Oxysterol-binding family protein
MSAP	P13M25-140-T	C08	38.8	Transcription factor Sox-5	

Table S7   List of consensus QTLs detected in G-map

Table S7 is available for download a compressed Excel file at
http://www.genetics.org/content/suppl/2011/09/02/genetics.111.131615.DC1.

Table S8 Consensus QTL distribution in I-map

Linkage group	Epigenetic		Genetic	
	QTLepi-c	QTLepi-l	QTLdna	QTLdna-l
A01(107.8)*	3	4	8	9
A02(120.4)	1	5	5	14
A03(135.4)	2	4	22	5
A04(112.1)	2	2	1	2
A05(158.3)	1	1	2	1
A06(149.3)	0	4	1	2
A07(134.5)	1	1	1	3
A08(89)	2	1	4	1
A09(131.2)	2	2	10	2
A10(83.2)	0	3	9	4
C01(64.1)	1	1	2	0
C02(125.1)	1	1	4	3
C03(157.3)	2	3	13	7
C04(140.5)	0	0	2	0
C05(143.1)	1	4	5	1
C06(113.4)	3	2	10	6
C07(114)	0	0	7	2
C08(130.5)	7	1	1	3
C09(135.5)	0	1	3	0
Total	**29**	**40**	**110**	**65**

* Genetic length of linkage group

Table S9   Number of different types of QTL controlling various traits detected from I-map

Trait	Number of environment	Mean primary QTL detected from a single environment		Total consensus QTL detected from all environments		Index of environmental specificity[◇]	
		QTLepi	QTLdna	QTLepi	QTLdna	QTLepi	QTLdna
Plant height	7	1.7	3.9	9	23	0.75	0.85
Oil content	4	2.3	8.8	9	32	1	0.91
Erucic acid content	4	2.5	4.5	2	8	0.2	0.44
Protein content	3	1.7	4.3	5	13	1	1
Seed developing time	10	3.3	5.3	12	32	0.36	0.6
Flowering time	10	4.2	7.6	17	30	0.4	0.39
Maturity time	10	2.8	5.2	15	37	0.54	0.71
Total	**48**	**18.4**	**39.5**	**69**	**175**	**0.61**	**0.7**

[◇] The index is the ratio of the total number of integrated consensus QTL and the total number of primary QTL for each trait.